

Spin injection into a metal from a topological insulator

S. Modak⁽¹⁾, K. Sengupta⁽¹⁾, and Diptiman Sen⁽²⁾

⁽¹⁾*Theoretical Physics Department, Indian Association for the Cultivation of Science, Jadavpur, Kolkata 700 032, India*

⁽²⁾*Center for High Energy Physics, Indian Institute of Science, Bangalore 560 012, India*

(Dated: February 27, 2013)

We study a junction of a topological insulator with a thin two-dimensional (2D) non-magnetic or partially polarized ferromagnetic metallic film deposited on a 3D insulator. We show that such a junction leads to a finite spin current injection into the film whose magnitude can be controlled by tuning a voltage V applied across the junction. For ferromagnetic films, the direction of the component of the spin current along the film magnetization can also be tuned by tuning the barrier potential V_0 at the junction. We point out the role of the chiral spin-momentum locking of the Dirac electrons behind this phenomenon and suggest experiments to test our theory.

PACS numbers: 73.20.-r, 73.40.-c, 71.10.Pm

Topological insulators (TI), a class of three-dimensional (3D) insulators with strong spin-orbit coupling, are known to possess gapless Dirac-like quasiparticles on their surfaces whose existence originates from the special topological properties of their bulk bands [1–9]. Such insulators, which are essentially 3D generalizations of their 2D counterparts which exhibit the quantum spin-Hall effect, have attracted a lot of theoretical and experimental attention in recent years. These TIs can be classified as strong or weak depending on their sensitivity to time reversal symmetric perturbations. The surfaces of the strong TIs have an odd number of Dirac cones; the number and positions of these cones depend on the nature of the surface concerned [1, 2, 4]. The odd number of the Dirac cones ensures that any surface impurity which conserves time reversal symmetry does not destroy the low-energy Dirac properties of the quasiparticles on the surface. For several compounds such as Bi_2Te_3 and Bi_2Se_3 , specific surfaces have been found with a single Dirac cone near the Γ point of the 2D surface Brillouin zone [2, 7, 9].

A Dirac cone on the surface of a TI is described by the Hamiltonian

$$H_{\hat{n}}[v_F] = \int \frac{dk_i dk_j}{(2\pi)^2} \psi_k^\dagger (\hbar v_F \hat{n} \cdot \vec{\sigma} \times \vec{k} - \mu I) \psi_{\vec{k}}, \quad (1)$$

where $\vec{\sigma}(I)$ denotes the Pauli (identity) matrices in spin space, \hat{n} denotes the unit vector normal to the TI surface which hosts electrons with momentum components k_i and k_j , v_F is the Fermi velocity, μ is the chemical potential, and $\psi = (\psi_\uparrow, \psi_\downarrow)^T$ is the annihilation operator for the Dirac spinor [10]. In this notation, \uparrow (\downarrow) denotes components of the quasiparticle spin along (opposite to) \hat{z} . Recently, several novel features of these surface Dirac electrons have been studied. These include the existence of Majorana fermions in the presence of a magnet-superconductor interface on the surface [10, 11], generation of a state resembling a $p_x + ip_y$ -wave superconductor but with time reversal symmetry via proximity to a s -wave superconductor [10], anomalous magnetoresis-

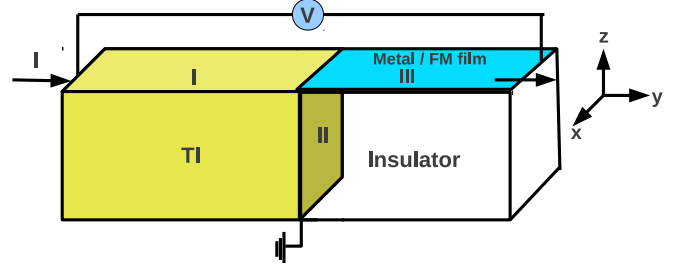


FIG. 1: (Color online) Schematic picture of the proposed junction. The two interfaces I and II of the topological insulator have low-energy quasiparticles with Dirac-like properties while the non-magnetic/ferromagnetic metallic thin film III deposited atop the insulator has conventional electrons obeying the Schrödinger equation. See text for details.

tance of ferromagnet-ferromagnet junctions [12], realization of a magnetic switch in junctions of these materials [13], spin textures with chiral properties [9], control of spin transport and polarization using gate voltages and electric fields [14, 15], realization of a Lifshitz transition in thin TI films [16], and spin-polarized STM spectra [17]. However, junctions of such TIs with conventional metals and ferromagnets have not been studied so far.

In this Letter, we study the transport properties of a junction of a TI with a conventional insulator with a non-magnetic or partially polarized ferromagnetic metallic film deposited on it as schematically shown in Fig. 1. The regions I and II in Fig. 1 refer to the two surfaces of the TI which host chiral Dirac quasiparticles, while region III consists of conventional electrons obeying the Schrödinger equation. We show that due to the chiral spin-momentum locking of the Dirac electrons on the surfaces of the TI, the transport through such a junction can lead to a finite spin current in the film without any skew scattering which is necessary in conventional spin-Hall materials to generate such currents. The magnitude of the spin current generated can be controlled by a voltage V applied across the junction *without the in-*

volvement of any external magnetic field. We also study the dependence of this spin current on the barrier potential V_0 at the junction and show that it displays an oscillatory feature with a decaying envelope as a function of V_0 . This behavior draws from both the chiral nature of the Dirac quasiparticles in regions I and II which leads to the oscillatory nature of the spin current [18], and the presence of the conventional Schrödinger electrons in region III which leads to an exponential decay of the spin current with increasing V_0 . Finally, we demonstrate that for ferromagnetic films, the direction of the component of the spin current along the film magnetization (J_z) can be controlled by tuning V_0 . To the best of our knowledge, the generation of spin current using the chirality of the Dirac quasiparticles on the surface of the TIs *whose direction and magnitude can both be controlled electrically* has not been proposed before; we therefore expect our proposal to generate significant interest in the field of spintronics.

We begin with the analysis of the junction in Fig. 1 when $V_0 = 0$. In region I, the Hamiltonian for the Dirac quasiparticles is given by Eq. (1) with $\hat{n} = \hat{z}$. The wave function for these quasiparticles with a transverse momenta k_x and energy $\epsilon = eV$ moving along $\pm \hat{y}$ can be obtained by solving the Dirac equation $H_{\hat{z}}[v_1]\psi_1 = \epsilon\psi_1$ and is given by $\psi_{\pm} = [1, -i \exp(\pm i\theta_k)]^T \exp[i(k_x x \pm k_y y)]/\sqrt{2}$, where $\theta_k = \arccos[\hbar v_1 k_x / (\epsilon + \mu)]$, $\epsilon = -\mu + \hbar v_1 \sqrt{k_x^2 + k_y^2}$, and v_1 is the Fermi velocity of the quasiparticles in region I. The wave function of the Dirac quasiparticles in region I can thus be written as

$$\psi_I = \psi_+ + r\psi_-, \quad (2)$$

where r is the reflection amplitude. We note that for any incident angle θ , ψ_+ and ψ_- have $\langle \psi_+ | \sigma_x | \psi_+ \rangle = \sin(\theta_k) = -\langle \psi_- | \sigma_x | \psi_- \rangle$. Thus the reflected Dirac quasiparticle has the opposite spin orientation along \hat{x} compared to its incident counterpart. This phenomenon is reminiscent of Andreev reflection from a superconducting junction where the charge and the transverse momenta of the reflected quasiparticle change sign. In contrast, for the junctions considered here, the transverse in-plane component of the quasiparticle spin changes sign upon reflection. In what follows, we shall show that this spin reversal is at the heart of the generation of a finite spin current in region III.

In region II, $\hat{n} = \hat{y}$, and the wave function of the Dirac quasiparticles moving along $-\hat{z}$ with transverse momenta k_x and energy ϵ can be obtained by solving $H_{\hat{y}}[v_2]\psi_2 = \epsilon\psi_2$ and is given by

$$\psi_{II} = t_1\psi_2, \quad \psi_2 = [u_k, v_k]^T e^{i(-k_z z + k_x x)}/\sqrt{2}, \quad (3)$$

where $u_k[v_k] = \sqrt{1 + [-] \cos(\phi_k)}$, $\phi_k = \arccos[\hbar v_2 k_x / (\epsilon + \mu)]$, $\epsilon = -\mu + \hbar v_2 \sqrt{k_z^2 + k_x^2}$, $v_2 = \beta^2 v_1$ is the Fermi velocity, and t_1 denotes the transmission

probability of the Dirac quasiparticles in region II. In the rest of this work, we shall choose $\beta = \sqrt{v_2/v_1} \leq 1$.

In the metallic film (region III), the Hamiltonian for the electrons can be written as $H_{III} = \hbar^2(k_x^2 + k_y'^2)/(2m) - \mu - A\sigma_z$, where μ and m are the chemical potential and mass of the electrons in the film, and A is proportional to the magnetization of the electrons. For a non-magnetic film $A = 0$, while for a fully polarized ferromagnetic film $A \rightarrow \infty$. In what follows, we first consider a non-magnetic film for which $A = 0$. The wave function of the electrons in region III is then given by

$$\psi_{III} = [t_2, t_3]^T e^{i(k_x x + k_y' y)}/\sqrt{2}, \quad (4)$$

where $\epsilon = -\mu + \hbar^2(k_x^2 + k_y'^2)/(2m)$, and t_2 and t_3 denote the transmission amplitudes of spin-up and spin-down electrons in region III.

The boundary condition on these wave functions involves continuity of current through the junction which yields

$$v_1 \psi_I^\dagger \sigma_x \psi_I - v_2 \psi_{II}^\dagger \sigma_x \psi_{II} = \frac{\hbar}{m} \text{Im}(\psi_{III}^\dagger \partial_y \psi_{III}), \quad (5)$$

where it is understood that all fields are evaluated at the junction line $y = 0$ (for ψ_I and ψ_{III}) and $z = 0$ (for ψ_{II}). We note that the unusual boundary condition (Eq. 5) in which a current without derivatives in regions I and II (Dirac equation) has to be matched with a current involving a first derivative in region III (Schrödinger equation) is generic for any junction involving a TI and a conventional material. (The situation here is different from a junction of ordinary materials with spin-orbit coupling where the current involves a first derivative on both sides [19]). Below, we present a general solution to this problem with (discussed in Eq. (14) below) and without a barrier potential [20].

In the absence of any barriers at the junction, the general solution of Eq. (5) is given by two linear conditions on the wave functions [21],

$$\psi_{III} = c(\psi_I + \beta\psi_{II}), \quad \frac{\hbar}{m} \partial_y \psi_{III} = \frac{iv_1 \sigma_x}{c} [\psi_I - \beta\psi_{II}], \quad (6)$$

where c is an arbitrary real constant; we will set $c = 1$ for simplicity. Note that the metal/ferromagnet decouples from the TIs for $c \rightarrow 0$ or ∞ . Substituting Eqs. (2-4) in Eq. 6, we obtain the following relations between r , t_1 , t_2 , and t_3 ,

$$\begin{aligned} 1 + r + (-)\beta u_k t_1 &= t_2(\alpha t_3), \\ e^{i\theta_k} + r e^{-i\theta_k} + (-)i\beta v_k t_1 &= it_3(i\alpha t_2), \end{aligned} \quad (7)$$

where $\alpha = \hbar k_y'/(mv_1)$. Solving for r , $t_{1,2,3}$ from Eq. (7), we get

$$\begin{aligned} r &= \mathcal{N}/\mathcal{D}, \quad t_1 = 2(1 - \alpha^2) \sin(\theta_k)/(\beta\mathcal{D}), \\ t_2 &= \frac{4}{\mathcal{D}} \sin(\theta_k)(u_k + \alpha v_k), \quad t_3 = \frac{4}{\mathcal{D}} \sin(\theta_k)(v_k + \alpha u_k), \end{aligned} \quad (8)$$

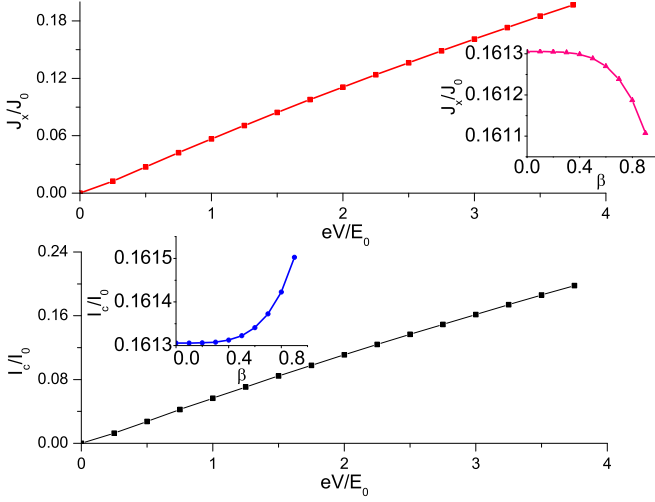


FIG. 2: (Color online) Plot of J_x (top panel) and I_c (bottom panel) in a non-magnetic metallic film as a function of V for $\beta = 1$. The insets show their β dependence for $eV/E_0 = 3$.

where $\mathcal{N} = -iu_k[\exp(i\theta_k)(1 + \alpha^2) - 2i\alpha] - v_k[(1 + \alpha^2) + 2i\alpha \exp(i\theta_k)]$, and $\mathcal{D} = i[u_k(1 + \alpha^2) + 2\alpha v_k] \exp(-i\theta_k) + v_k(1 + \alpha^2) + 2\alpha u_k$.

Eq. (8) predicts a net spin current along \hat{x} in the metallic region: $J_x = (\hbar v_1/2) \sum_{k_x} \langle \psi_{III} | \alpha \sigma_x | \psi_{III} \rangle = (\hbar v_1/2) \sum_{k_x} \alpha (t_2^* t_3 + \text{h.c.})$. This can be written as

$$J_x = \frac{8J_0}{\pi} \int_{-E/(2E_0)}^{E/(2E_0)} dx \frac{\alpha[(1 + \alpha^2) \sin(\phi_k) + \alpha] \sin^2(\theta_k)}{|\mathcal{D}|^2}, \quad (9)$$

where $J_0 = \hbar v_1 k_0$, $x = k_x/k_0$, $k_0 = mv_1/\hbar$, $E = eV + \mu$, and $E_0 = \hbar v_1 k_0/2$. A plot of J_x/J_0 as a function of the applied voltage eV/E_0 , shown in the bottom panel of Fig. 2, confirms that the net spin current is finite and its amplitude depends on V . The inset shows the dependence of the spin current on β for a fixed V and confirms the presence of a finite J_x for the entire range of $0 < \beta \leq 1$. The charge current is given by $I_c = ev_1 \sum_{k_x} \alpha (|t_2|^2 + |t_3|^2)$ which can be written as

$$I_c = \frac{4I_0}{\pi} \int_{-E/(2E_0)}^{E/(2E_0)} dx \frac{\alpha[1 + \alpha^2 + 2\alpha \sin(\phi_k)] \sin^2(\theta_k)}{|\mathcal{D}|^2}, \quad (10)$$

where $I_0 = ev_1 k_0$. The top panel of Fig. 2 shows the variation of I_c/I_0 with the applied voltage V , while the inset depicts its variation with β . We note that the charge current displays a qualitatively similar behavior as the spin current along \hat{x} . The net spin current along y and z vanishes. For J_z this can be seen by noting that $u_k \rightarrow v_k$ under $k_x \rightarrow -k_x$. Consequently $t_2 \rightarrow t_3$ under this transformation which leads to a zero net value for $J_z \sim \sum_{k_x} \alpha (|t_2|^2 - |t_3|^2)$. Also, using the fact that t_2 and t_3 are both purely imaginary (Eq. (8)), it can be easily shown that $J_y = 0$ [22].

Next, we address the behavior of the spin and charge

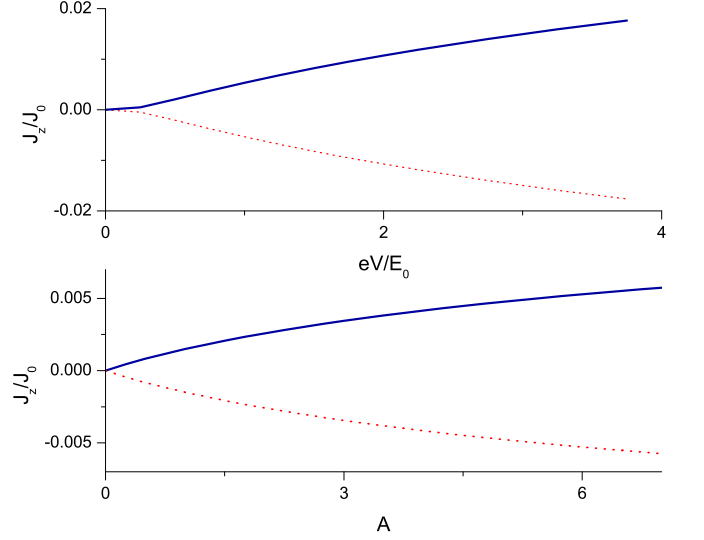


FIG. 3: (Color online) Plot of J_z versus eV when $\mu = A$ (red dashed line) and $\mu = -A$ (blue solid line) for $A/E_0 = 3$ (top panel) and as a function of A (bottom panel) for $\beta = 1$ and $eV/E_0 = 3$ and $\mu = A$ (red dashed line) and $\mu = -A$ (blue solid line).

currents for a ferromagnetic film where $A \neq 0$. In this case, the wave function in region III is given by

$$\psi_{III}^{\text{FM}} = [t_2 e^{ik_y^{(1)}y}, t_3 e^{ik_y^{(2)}y}]^T e^{ik_x x} / \sqrt{2}, \quad (11)$$

where $k_y^{(1) [(2)]} = [2m(\epsilon + \mu + [-]A)/\hbar^2 - k_x^2]^{1/2}$. The boundary condition on the wave function is given by Eq. (6) and yields

$$t_{2[3]} = -4ie^{i\theta_k} \sin(\theta_k) (u_k[\alpha_2 u_k] + \alpha_1 v_k[v_k]) / \mathcal{D}_1, \quad (12)$$

where $\alpha_{1(2)} = \hbar k_y^{(1)} (k_y^{(2)}) / (mv_1)$, and $\mathcal{D}_1 = p_1 - ip_2 \exp(i\theta_k)$, where $p_1 = u_k(1 + \alpha_1 \alpha_2) + 2v_k \alpha_2$, and $p_2 = v_k(1 + \alpha_1 \alpha_2) + 2u_k \alpha_2$. Note that for $A = 0$, $\alpha_1 = \alpha_2 = \alpha$; in this limit Eq. (12) matches with Eq. (8). Using this wave function, it is straightforward to compute the expression for I_c following the method outlined earlier which shows qualitatively similar behavior as in metallic films.

The key difference between the ferromagnetic and the non-magnetic films which we now focus on is that the former films allow a non-zero J_z . This is easily seen from Eq. (12) by noting that $t_2(k_x) \neq t_3(-k_x)$ due to the difference of velocities of the up and the down spin quasiparticles; this leads to a finite J_z in region III given by

$$J_z = \frac{J_0}{2\pi} \int_{-E/(2E_0)}^{E/(2E_0)} dx (\alpha_1 |t_2|^2 - \alpha_2 |t_3|^2). \quad (13)$$

In what follows, we set $\mu = A$ or $\mu = -A$ so that the spin-up or spin-down Fermi surface is aligned with the Fermi surface in region I. Increasing A therefore pushes

the other Fermi surface away from the Fermi surface of region I and hence increases the effective spin polarization of the film in region III. The behavior of J_z , computed by substituting Eq. (12) in Eq. (13), is shown in Fig. 3. The top panel of the figure shows the variation of J_z as a function of eV/E_0 for $A/E_0 = 3$, while the bottom panel shows the dependence of J_z on A for fixed $eV/E_0 = 3$ and $\beta = 1$. These plots demonstrate the presence of a finite J_z for a large range of V ; the sign of J_z depends on the magnetization of the film while its magnitude can be controlled by the applied voltage V .

Next, we consider the effect of a finite barrier potential V_0 applied over a region d at the junction. In what follows we will consider the thin-barrier limit where $V_0 \rightarrow \infty$ and $d \rightarrow 0$ keeping $\chi = V_0 d / (\hbar v_1)$ finite. In this limit, the boundary condition to be imposed on the wave functions reads [21, 23]

$$\psi_{III} = e^{-i\chi\sigma_x}\psi_I + \beta e^{i\chi\sigma_x/\beta^2}\psi_{II}, \quad (14)$$

$$\frac{\hbar}{mv_1}\partial_y\psi_{III} - 2\chi\psi_{III} = i\sigma_x(e^{-i\chi\sigma_x}\psi_I - \beta e^{i\chi\sigma_x/\beta^2}\psi_{II}).$$

Substituting Eqs. (2), (3), and (11) in Eq. (14), we again obtain a set of four equations for r and $t_{1,2,3}$ which reads

$$\begin{aligned} t_{2[3]} &= \frac{1}{\sqrt{2}}(a_1[ia_2] + ra_1^*[ia_2^*] + [-]\beta t_1 b_1[b_2]), \\ (\alpha_{1[2]} + 2i\chi)t_{3[2]} &= \frac{1}{\sqrt{2}}(a_1[-ia_2] + ra_1^*[-ia_2^*] - \beta t_1 b_1[b_2]) \end{aligned}$$

where $a_1 = \cos(\chi) - \sin(\chi)\exp(i\theta_k)$, $a_2 = \sin(\chi) + \cos(\chi)\exp(i\theta_k)$, and $b_{1[2]} = u_k[v_k]\cos(\chi/\beta^2) + iv_k[u_k]\sin(\chi/\beta^2)$. The solution of these equations yields

$$t_{2[3]} = [-2(b_{1[2]} + b_{2[1]})(\alpha_{1[2]} + 2i\chi)(a_1^*a_2 - a_2^*a_1)]/\mathcal{D}_2, \quad (15)$$

where $\mathcal{D}_2 = [-2b_1(2\chi + i\alpha_1) + b_2\{-1 + (\alpha_1 - 2i\chi)(\alpha_2 - 2i\chi)\}]a_1 + [b_1(1 + (\alpha_1 + 2i\chi)(\alpha_2 + 2i\chi)) + 2b_2(\alpha_2 + 2i\chi)]a_2^*$ for magnetic films. The corresponding expressions for the non-magnetic films can be obtained by putting $\alpha_1 = \alpha_2$ in Eq. (15). We note that Eq. (15) reproduces Eq. (12) for $\chi = 0$.

From Eq. (15), we find that the barrier potential χ enters the transmission amplitudes $t_{2[3]}$ both through the $\cos(\chi)$ and $\sin(\chi)$ factors in $a_{1(2)}$ and $b_{1(2)}$ leading to an oscillatory χ dependence of $t_{2(3)}$ and through the appearance of χ in the numerator and denominator of Eq. (15), which, in the limit of large χ , leads to a decay of $t_{2(3)}$ with increasing χ . The former behavior arises from the Dirac nature of the electrons in regions I and II, while the latter is a consequence of the conventional Schrödinger nature of the electrons in region III. Consequently, we expect $t_{2(3)}$ to have an oscillatory dependence on χ along with a decaying envelope. We note that such a behavior is different from what is found in analogous junctions involving solely Dirac or solely conventional materials.

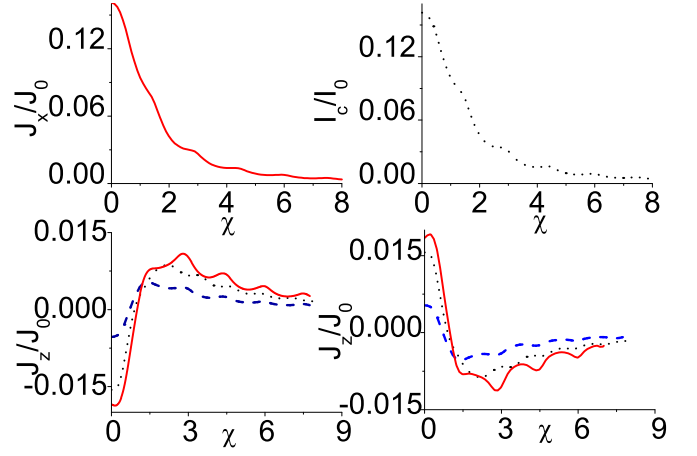


FIG. 4: (Color online) Top left (right) panel: Variation of J_x (I_c) with χ in a metallic film for $eV/E_0 = 3$. Bottom left (right) panel: Variation of J_z with χ in a ferromagnetic film for $\mu = A = 3E_0$ ($\mu = -A = -3E_0$) for $eV/E_0 = 4$ (red solid line), 3 (black dotted line) and 1 (blue dashed line). For all the plots $\beta = 1$.

To compute the spin and charge currents, we substitute the values of $t_{2(3)}$ from Eq. (15) in the expressions $J_z = \hbar v_1 \sum_{k_x} (\alpha_1 |t_2|^2 - \alpha_2 |t_3|^2)$ for ferromagnetic films, and $I_c = ev_1 \sum_{k_x} \alpha_1 (|t_2|^2 + |t_3|^2)$ and $J_x = \hbar v_1 \sum_{k_x} \alpha (t_3^* t_2 + \text{h.c.})$ for non-magnetic films. The resulting dependence of J_z , I_c and J_x on χ is shown in Fig. 4 for $\beta = 1$. The top panel shows the behavior of J_x and I_c for non-magnetic films for $eV/E_0 = 3$. We find that both J_x and I_c display small oscillatory features with an overall monotonic decay as a function of χ . We have found qualitatively similar behavior of J_x and I_c in magnetic films. In contrast, J_z for magnetic films, shown in the left (right) bottom panels of Fig. 4 for $\mu = A$ ($\mu = -A$) for several representative values of eV/E_0 displays a non-monotonic behavior with increasing χ . In particular, these plots demonstrate that the sign of the spin currents gets reversed with increasing χ which allows for the possibility of tuning the sign of J_z by tuning V_0 . This leads to electrical control of both the magnitude and the direction of J_z in magnetic films via tuning externally applied voltages V and V_0 .

To experimentally verify our theory, we propose measuring the current in region III for magnetic films using a ferromagnetic contact. When the direction of magnetization of the contact is along \hat{z} , it will measure only the current due to the spin-up electrons: $I_\uparrow = ev_1 \sum_{k_x} \alpha_1 |t_2|^2 = [I_c + eJ_z/(2\hbar)]/2$. Similarly a contact with magnetization along $-\hat{z}$ will record $I_\downarrow = [I_c - eJ_z/(2\hbar)]/2$. Thus the difference between these two currents will provide a measure of the spin current through the film as a function of the applied voltage V and the potential barrier V_0 : $J_z = 2\hbar(I_\uparrow - I_\downarrow)/e$. Thus such an experiment can verify the predicted dependence of J_z on V and V_0 [21].

In conclusion, we have studied a junction of a TI with

a thin metallic/partially polarized ferromagnetic film deposited over an ordinary insulator. For ferromagnetic films, we have shown that such a junction can be used to generate a finite spin current along \hat{z} whose magnitude and direction can both be controlled by externally applied voltages without the presence of any external magnetic field. Our work shows that the chiral spin-momentum locking of the Dirac quasiparticles on the surfaces of the TI is at the heart of this phenomenon. Finally, we have suggested a simple experiment to test our theory.

K.S. and D.S. thank DST, India for financial support through grants SR/S2/CMP-0001/2009 and SR/S2/JCB-44/2010 respectively.

-
- [1] B. A. Bernevig, T. L. Hughes, and S.-C. Zhang, *Science* **314**, 1757 (2006); B. A. Bernevig and S.-C. Zhang, *Phys. Rev. Lett.* **96**, 106802 (2006).
 - [2] M. Koenig *et al.*, *Science* **318**, 766 (2007); D. Hsieh *et al.*, *Nature* **452**, 970 (2008).
 - [3] C. L. Kane and E. J. Mele, *Phys. Rev. Lett.* **95**, 226801 (2005); *ibid.*, *Phys. Rev. Lett.* **95**, 146802 (2006).
 - [4] L. Fu, C. L. Kane, and E. J. Mele, *Phys. Rev. Lett.* **98**, 106803 (2007); R. Roy, *Phys. Rev. B* **79**, 195322 (2009); J. E. Moore and L. Balents, *Phys. Rev. B* **75**, 121306 (2007).
 - [5] J. C. Y. Teo, L. Fu, and C. L. Kane, *Phys. Rev. B* **78**, 045426 (2008).
 - [6] X. L. Qi, T. L. Hughes, and S. C. Zhang, *Phys. Rev. B* **78**, 195424 (2008); H. Zhang *et al.*, *Nature Phys.* **5**, 438 (2009).
 - [7] Y. Xia *et al.*, *Nature Phys.* **5**, 398 (2009); *ibid.*, arXiv:0907.3089 (unpublished).
 - [8] Y. L. Chen *et al.*, *Science* **325**, 5937 (2009); T. Zhang *et al.*, arXiv:0908.4136v3 (unpublished).
 - [9] D. Hsieh *et al.*, *Nature* **460**, 1101 (2009); P. Roushan *et al.*, *Nature* **460**, 1106 (2009); D. Hsieh *et al.*, *Science* **323**, 919 (2009).
 - [10] L. Fu and C. L. Kane, *Phys. Rev. Lett.* **100**, 096407 (2008).
 - [11] A. R. Akhmerov, J. Nilsson, and C. W. J. Beenakker, *Phys. Rev. Lett.* **102**, 216404 (2009); Y. Tanaka, T. Yokoyama, and N. Nagaosa, *Phys. Rev. Lett.* **103**, 107002 (2009); J. Linder *et al.*, *Phys. Rev. Lett.* **104**, 067001 (2010).
 - [12] T. Yokoyama, Y. Tanaka, and N. Nagaosa, *Phys. Rev. Lett.* **102**, 166801 (2009).
 - [13] S. Mondal *et al.*, *Phys. Rev. Lett.* **104**, 046403 (2010); *ibid.*, *Phys. Rev. B* **82**, 045120 (2010).
 - [14] A. A. Burkov and D. G. Hawthorn, *Phys. Rev. Lett.* **105**, 066802 (2010); O. V. Yazyev, J. E. Moore, and S. G. Louie, *Phys. Rev. Lett.* **105**, 266806 (2010); K. Nomura and N. Nagaosa, *Phys. Rev. B* **82**, 161401 (2010); T. Yokoyama, J. Zang, and N. Nagaosa, *Phys. Rev. B* **81**, 241410(R) (2010).
 - [15] I. Garate and M. Franz, *Phys. Rev. Lett.* **104**, 146802 (2010); *ibid.*, *Phys. Rev. B* **81**, 172408 (2010).
 - [16] A. A. Zyuzin, M. D. Hook, and A. A. Burkov, *Phys. Rev. B* **83**, 245428 (2011).

- [17] K. Saha *et al.*, *Phys. Rev. B* **89**, 123456 (2011).
- [18] The oscillatory behavior of charge current with barrier voltage but without the decaying profile has been predicted for Dirac quasiparticles in graphene; see S. Bhattacharjee and K. Sengupta, *Phys. Rev. Lett.* **97**, 217001 (2006).
- [19] L. W. Molenkamp, G. Schmidt, and G. E. W. Bauer, *Phys. Rev. B* **64**, 121202(R) (2001).
- [20] Note that such a matching can only be done in the presence of a Dirac cone in region II since it is crucial for providing the exact match between the number of states for the Dirac electrons (one state per spin) with the Schrödinger electrons in the metal/ferromagnet (two states per spin).
- [21] See Supplemental Material for a derivation of the boundary conditions at the junction and for numerical estimates of the currents to be measured.
- [22] The origin of a finite J_x in the non-magnetic film can be easily traced back to the helicity of the Dirac electrons which leads to a reversal of the electron spin along \hat{x} upon reflection from the interface.
- [23] D. Sen and O. Deb, *Phys. Rev. B* **85**, 245402 (2012).

APPENDIX A

In this Section, we provide some supplemental material to the main text related to the derivation of the boundary condition Eq. 14 and numerical estimate of the measured current in suggested experiment.

Current conserving boundary conditions at a junction

In this section, we will find the general time reversal invariant boundary condition which satisfies the current conservation relation at the junction discussed in our paper. We begin with the Hamiltonians in the three regions. Region I of the topological insulator (TI) is defined by the half-plane $z = 0$ and $y < 0$, and has the Dirac Hamiltonian

$$H_I = i\hbar v_1 [-\sigma_x \partial_y + \sigma_y \partial_x]. \quad (16)$$

Region II of the TI, given by the half-plane $y = 0$ and $z < 0$, has the Hamiltonian

$$H_{II} = i\hbar v_2 [-\sigma_z \partial_x + \sigma_x \partial_z]. \quad (17)$$

Region III of the non-magnetic metal/ferromagnet thin film is defined by the half-plane $z = 0$ and $y > 0$, and has the Schrödinger Hamiltonian

$$H_{III} = -\frac{\hbar^2}{2m} (\partial_x^2 + \partial_y^2) - \mu - A\sigma_z. \quad (18)$$

The time evolution equations $i\hbar \partial \psi_a / \partial t = H_a \psi_a$ ($a = I, II, III$) are invariant under time reversal ($t \rightarrow -t$ and

complex conjugation of all numbers) if $\psi_i \rightarrow \sigma_y \psi_i^*$ and $A = 0$.

The junction of the three regions is given by the line $y = z = 0$. The conservation of the total current coming into the junction from the three regions is given by Eq. (5) of our paper, namely,

$$v_1(\psi_I^\dagger \sigma_x \psi_I)_{y=0-} - v_2(\psi_{II}^\dagger \sigma_x \psi_{II})_{z=0-} = \frac{\hbar}{m} \text{Im}(\psi_{III}^\dagger \partial_y \psi_{III})_{y=0+}. \quad (19)$$

In order to satisfy this equation, let us assume linear relations between the wave functions at the junction of the form

$$\begin{aligned} (\psi_{III})_{y=0+} &= A_1(\psi_I)_{y=0-} + A_2(\psi_{II})_{z=0-}, \\ \frac{\hbar}{m} (\partial_y \psi_{III})_{y=0+} &= i\sigma_x [A_3(\psi_I)_{y=0-} + A_4(\psi_{II})_{z=0-}], \end{aligned} \quad (20)$$

where the A_i are four parameters. The relations in Eq. (20) will be time reversal invariant if the A_i are real. We can now check that Eq. (19) will be satisfied if $A_1 A_3 = v_1$, $A_2 A_4 = -v_2$ and $A_1 A_4 + A_2 A_3 = 0$. This implies that the A_i can be written in terms of a single real parameter c as $A_1 = c$, $A_2 = c\beta$, $A_3 = v_1/c$ and $A_4 = -v_1\beta/c$, where $\beta = \sqrt{v_2/v_1}$; this gives

$$\begin{aligned} (\psi_{III})_{y=0+} &= c[(\psi_I)_{y=0-} + \beta(\psi_{II})_{z=0-}], \\ \frac{\hbar}{m} (\partial_y \psi_{III})_{y=0+} &= \frac{iv_1\sigma_x}{c} [(\psi_I)_{y=0-} - \beta(\psi_{II})_{z=0-}], \end{aligned} \quad (21)$$

which is Eq. (6) of our paper. In the limits $c \rightarrow 0$ (or ∞), we obtain $\psi_{III} = 0$ (or $\partial_y \psi_{III} = 0$); in either case, the current into the junction from region III vanishes, so that the metal/ferromagnet gets decoupled from the two TI regions. The value of c in a given system will depend on its microscopic details such as an underlying lattice model. For the numerical calculations in our paper, we have simply set $c = 1$.

The above analysis assumed that there is no barrier present at the junction. A realistic system may be expected to have some potential barriers present at the junction in all three regions. Let us assume thin barriers of the form $V(y) = V_0$ for $-d < y < 0$ in region I, $V(z) = V_0$ for $-d < z < 0$ in region II, and $V(y) = V_0$ for $0 < y < d$ in region III. For simplicity, we have assumed the barrier width (d) and height (V_0) to be the same in all three regions; we will eventually be interested in the δ -function limit $d \rightarrow 0$ and $V_0 \rightarrow \infty$ keeping $dV_0/(\hbar v_1) = \chi$

constant. In Ref. ? , it has been shown that δ -function barrier in a Dirac Hamiltonian produces a discontinuity in the wave function of the form

$$\begin{aligned} (\psi_I)_{y=0-} &= e^{-i\chi\sigma_x} (\psi_I)_{y=-d}, \\ (\psi_{II})_{z=0-} &= e^{i\chi(v_1/v_2)\sigma_x} (\psi_{II})_{z=-d}. \end{aligned} \quad (22)$$

A δ -function barrier in a Schrödinger Hamiltonian produces no discontinuity in the wave function (i.e., $(\psi_{III})_{y=d} = (\psi_{III})_{y=0+}$), but there is a discontinuity in the first derivative of the form

$$\frac{\hbar}{m} [(\partial_y \psi_{III})_{y=d} - (\partial_y \psi_{III})_{y=0+}] = 2\chi v_1 (\psi_{III})_{y=d}. \quad (23)$$

Substituting Eqs. (22-23) in Eq. (21), and setting $c = 1$, we obtain

$$\begin{aligned} (\psi_{III})_{y=d} &= e^{-i\chi\sigma_x} (\psi_I)_{y=-d} + \beta e^{i(\chi/\beta^2)\sigma_x} (\psi_{II})_{z=-d}, \\ \frac{\hbar}{m} (\partial_y \psi_{III})_{y=d} - 2\chi v_1 (\psi_{III})_{y=d} &= iv_1\sigma_x [e^{-i\chi\sigma_x} (\psi_I)_{y=-d} - \beta e^{i(\chi/\beta^2)\sigma_x} (\psi_{II})_{z=-d}]. \end{aligned} \quad (24)$$

In the limit $d \rightarrow 0$, this gives Eq. (14) of our paper.

Numerical estimates of measured currents

In this section we provide estimates for I_\uparrow and I_\downarrow which are to be measured in the proposed experiment. For a typical TI surface, the group velocity of the Dirac electrons turns out to be $v_1 \sim 10^6$ m/s. This gives us an estimate of $k_0 = mv_1/\hbar \simeq 8.63 \times 10^{-9} \text{m}^{-1}$. Using this, one finds $I_0 = ev_1 k_0 \simeq 13.83 \text{mA}$ and $E_0 = mv_1^2/2 \simeq 2.89 \text{eV}$. Since I_\uparrow and I_\downarrow can be written as

$$I_{\uparrow(\downarrow)} = \frac{4I_0}{\pi} \int_{-E/(2E_0)}^{E/(2E_0)} dx \alpha_1 |t_2|^2 (\alpha_2 |t_3|^2), \quad (25)$$

we find numerical values of $I_\uparrow = 0.113 \text{mA}$ and $I_\downarrow = 0.0906 \text{mA}$ for $\chi = 0$ and $\mu = -A = 3E_0$. This indicates that the visibility V defined by

$$V = \left| \frac{I_\uparrow - I_\downarrow}{I_\uparrow + I_\downarrow} \right| \quad (26)$$

is close to 0.1 which means that such current measurements are well within the reach of current experimental standards. For finite and large barrier strength $\chi = 5$, the corresponding numbers are $I_\uparrow = 0.0068 \text{mA}$ and $I_\downarrow = 0.012 \text{mA}$ which leads to $V \simeq 0.28$.